Recommendations for the Design of Differential Thin-Film Microstrip Lines

Gia Ngoc Phung, Uwe Arz
Physikalisch-Technische Bundesanstalt
Bundesallee 100
38116 Braunschweig, Germany
{gia.phung@ptb.de, uwe.arz@ptb.de}

Thi Dao Pham, Djamel Allal
Laboratoire national de métrologie et d'essais
29 Avenue Roger Hennequin
78197 Trappes Cedex, France
{thi-dao.bui,djamel.allal@lne.fr}

Khitem Lahbacha, Gianfranco Miele, Antonio Maffucci
University of Cassino and Southern Lazio
Via G. Di Biasio 43
03043 Cassino (FR), Italy
{khitem.lahbacha,g.miele,maffucci@unicas.it}

Abstract—**Reliable high-speed data transmission and high-speed electronic components require a high level of Signal Integrity (SI) to handle hundreds of channels and thousands of input/output connections on a single chip. Due to the increasing demand for high-density layouts on a single chip, crosstalk effects are becoming critical for the system performance. This paper investigates crosstalk effects for coupled thin-film microstrip lines (TFMSL) in the frequency range up to 50 GHz. Neighborhood effects on the propagation characteristics of the common and the differential modes and mode conversion losses are discussed, and furthermore recommendations for the mitigation of unwanted effects are provided.**

Index Terms—**thin-film microstriplines, parasitic effects, electromagnetic (EM) simulation**

I. INTRODUCTION

Signal integrity (SI) and power integrity (PI) have been well-established technical areas for decades and are becoming increasingly important as the operating frequency, i.e., bit rate, of high-speed digital circuits such as e.g. field programmable gate array (FPGA) chips increases. With higher operating frequencies, the demand for high-density layouts and miniaturization on a single chip also increases. Therefore, it is of fundamental importance to understand the underlying phenomena of crosstalk effects, especially for differential transmission lines, which are commonly used in many end-user RF systems.

For more than two decades, major efforts have been made to develop calibration algorithms for the measurement of differential devices, e.g., the multimode Thru Reflect Line (TRL) calibration [1],[2],[3] and the simplified approach based on TRL calibration [4]. Previous work has investigated differential line standards on a reference printed circuit board (PCB) [5] and differential coplanar waveguides were also studied in [3], [6]. In [7] the impact of adjacent structures, bends and ground openings for single-ended differential thin-film microstrip lines with Ground-Signal-Ground (GSG) pads have been investigated using the multiline TRL algorithm [8].

This paper investigates crosstalk effects in differential thin-film microstrip lines (TFMSL) with Ground-Signal-Signal-Ground (GSSG) pads applying the multimode TRL algorithm [3] and discusses the impact of neighborhood effects on the calibrated propagation characteristics of the differential and the common modes. In addition, mode conversion losses from the differential to the common mode are also studied. The

TABLE I
TRANSMISSION LINE PARAMETERS

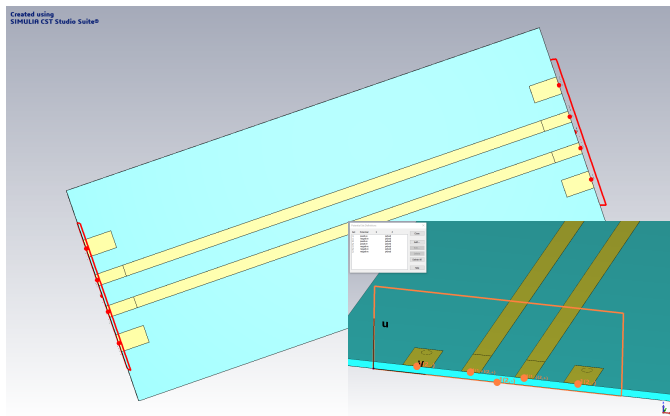| Parameter	Dimension (µm)
Pad width	80
Line width	52
Pitch size	150
Line length	5000
Pad length	130
Line thickness	0.5
Substrate thickness	20
Ground thickness	0.5

Fig. 1. Differential thin-film microstrip lines with GSSG pads excited with ideal waveguide ports.

goal of this work is to understand the crosstalk effects and to identify the parameters relevant to keep parasitic coupling to a minimum.

The test structures have been designed to allow focus on reflection, crosstalk and mode conversion effects. They are made of coupled transmission lines using thin-film microstrip line technology on SU-8 thin-film shown in Table I. Electromagnetic (EM) simulations were performed using the time domain solver in CST Microwave Studio [9]. In the EM simulation, the multipin port definition as shown in Fig. 1 is used to excite both modes, i.e. differential and common modes. To remove the GSSG pad effects, the multimode TRL algorithm based on [3] is applied to all calibrated data presented in this work.
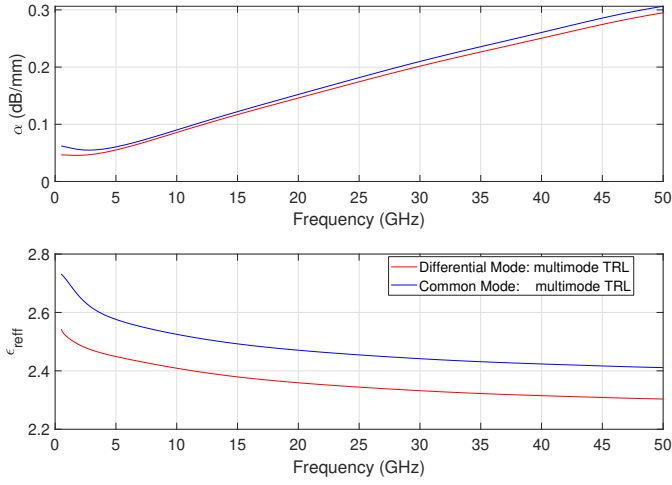
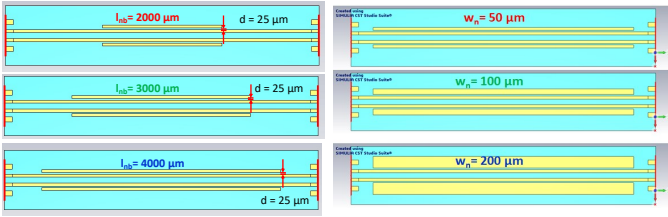Fig. 2. Propagation constants of the common and differential modes.

Fig. 3. Variation of the shape (length l_n and width w_n) of the adjacent structure.

II. MULTIMODE TRL CALIBRATION

The TRL calibration kit consists of a Thru with 0.5 mm length, a Line with 1 mm length and a short as reflect standard. The first results of the multimode TRL calibration are the propagation constants of the common and differential modes which are plotted in Fig. 2. When comparing the attenuation constant, only minor differences between the two modes can be detected. In contrast, the effective permittivity of the two modes exhibits larger deviations, as expected. Compared to the effective permittivity of the differential mode, the effective permittivity of the common mode is larger due to the stronger electric field concentration inside the substrate of the common mode.

III. IMPACT OF SYMMETRICAL ADJACENT STRUCTURES

The question now is how the transmission behavior and mode conversion losses of the investigated DUTs in common and differential operation are affected when symmetrical or asymmetrical neighbors are added.

In the following, the influence of symmetrical neighbors is investigated by adding lateral neighbors to the DUT, a differential line 5 mm long (excluding the pads). At first, the length l_n and the width w_n of the adjacent structure are varied as shown in Fig. 3. The results of the length and width variation of the adjacent structure are shown in Figs. 4 and 5.

As expected, the length of the adjacent structure is mainly responsible for the position of the resonant frequency due to
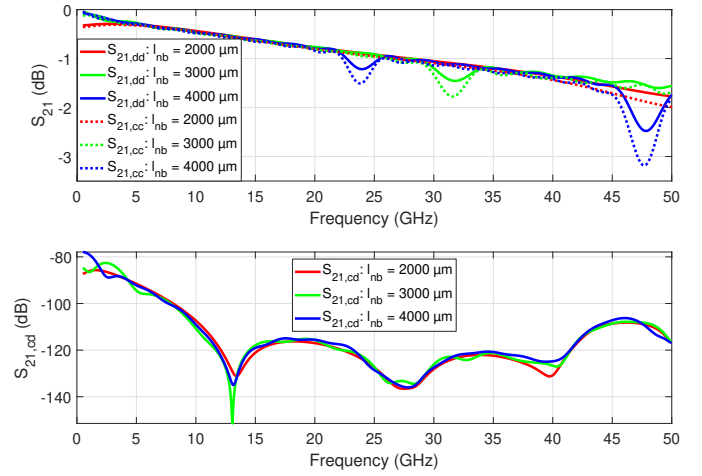

Fig. 4. Variation of line length l_n of the adjacent structure: Magnitude of simulated transmission coefficient $|S_{21}|$ for the common and differential modes and mode conversion losses $|S_{cd}|$ from the differential to common mode.
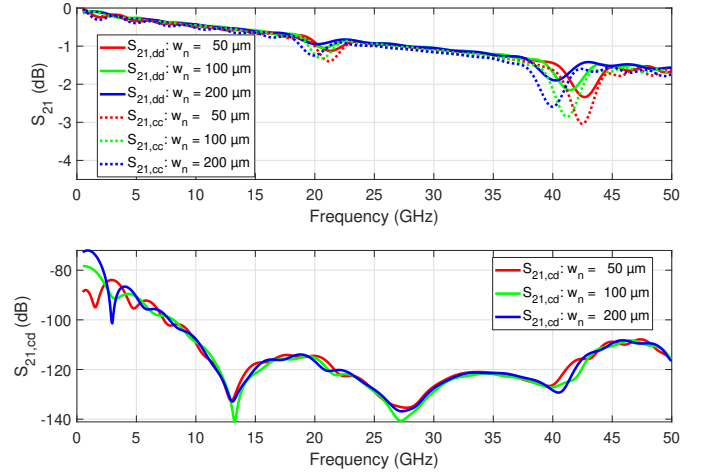

Fig. 5. Variation of width w_n of the adjacent structure: Magnitude of simulated transmission coefficient $|S_{21}|$ for the common and differential modes and mode conversion losses $|S_{cd}|$ from the differential to common mode.

the half-wavelength resonances for both modes. As the length of the adjacent structure increases, the resonant frequency decreases. Comparing the strength of the resonances of both modes, the common mode shows a much stronger resonant behavior than the differential mode. The magnitude of the mode conversion losses remains the same with varied lengths. However, it can be observed that the length of the adjacent structure also initiates ripples into the mode conversion losses.

The width of the adjacent structure changes the magnitude of the resonances and slightly shifts the resonant frequency. This shift in resonant frequency due to the wider adjacent structure can be explained by the increase in the effective permittivity as the electric fields become more concentrated inside the substrate. It is also interesting to note that the DUT with adjacent structures of smaller widths shows much stronger resonances than that of wider widths. For the mode conversion
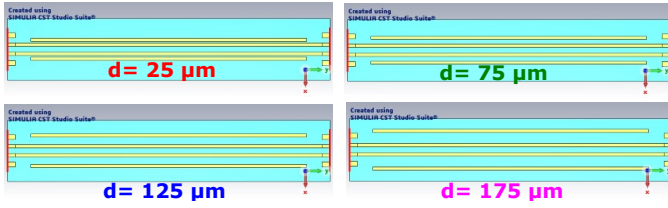
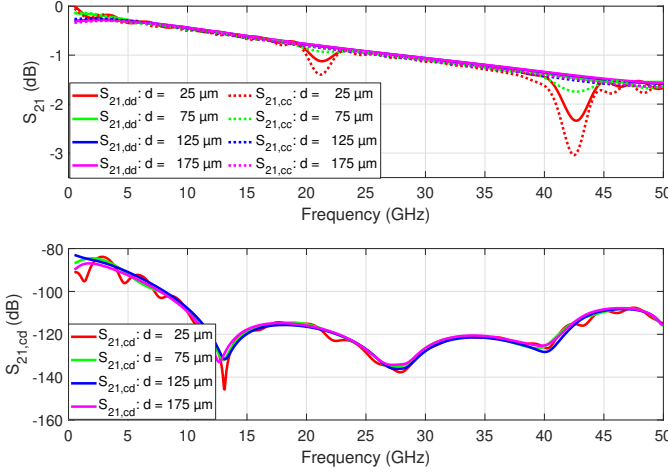Fig. 6. Varying distance d to the adjacent structure.

Fig. 7. Variation of distance d to the adjacent structure: Magnitude of simulated transmission coefficient $|S_{21}|$ for the common and differential modes and mode conversion losses $|S_{cd}|$ from the differential to common mode.

losses, a similar behavior as for the length variations can be observed.

After identifying the impact of the shape of the adjacent structure, the lateral distance between two adjacent structures on the transmission behavior of the two modes is investigated as shown in Fig. 6.

Comparing the results in Fig. 7, it is obvious that the resonance effects become weaker and finally disappear with larger distances for both modes. At a distance of $d = 125$ µm (almost 6.25 times the substrate thickness), an improved resonance behavior can be obtained for the investigated frequency range up to 50 GHz. The magnitude of the mode conversion losses is also not affected by the different distances. Small ripples can be observed in the curves of the mode conversion losses.

IV. Impact of Asymmetrical Adjacent Structures

So far, neighborhood effects have been studied for symmetrical DUTs. In most applications, e.g. FPGA, printed circuit boards or RF systems, symmetries in circuits usually cannot be fulfilled. It is therefore more important to understand what effects occur in asymmetrically-disturbed differential lines.

Fig. 8 shows the investigated DUTs. Fig. 9 compares the corresponding transmission coefficients to the symmetrical case whereas Fig. 10 shows the mode conversion losses.

Two physical effects can be observed here. Obviously, for both asymmetrical and symmetrical structures, it can be stated that the resonance behavior of the common mode is more

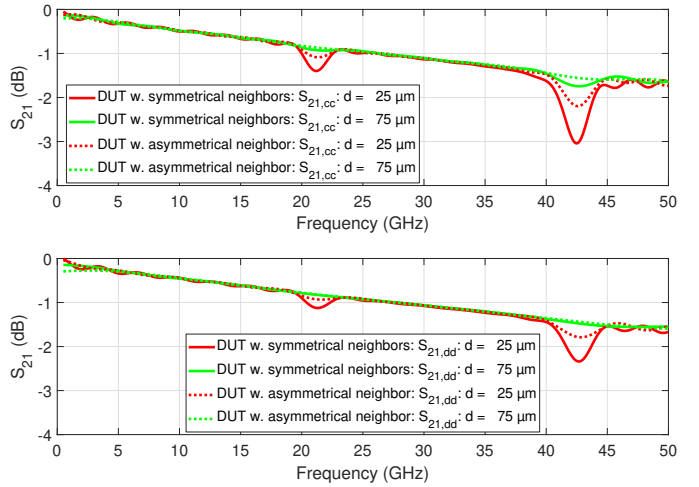Fig. 8. Investigated configuration of asymmetrical adjacent structures.

Fig. 9. Variation of distance d to the adjacent structure: Magnitude of simulated transmission coefficient $|S_{21}|$ for the common and differential modes.

strongly influenced by the adjacent structure than that of the differential mode.

While the transmission coefficients are less affected by the asymmetrical configurations, as expected the mode conversion losses are much more affected with values up to -22 dB. This clearly shows that energy leaks from the differential mode to the common mode due to the asymmetries: the smaller the distances, the stronger the effect.
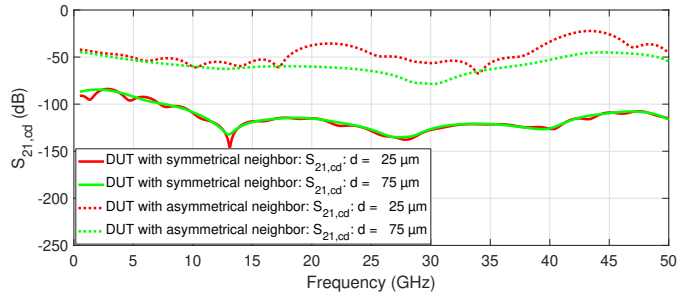

Fig. 10. Variation of distance d to the adjacent structure: Magnitude of simulated transmission coefficient $|S_{cd}|$ from the differential to the common mode.

V. Conclusion

When designing high-density layouts, it is important to understand the extent to which adjacent structures can contribute to parasitic effects or signal degradation.

In this paper, a thorough study of differential lines by EM simulations has led to the following findings:

- The length of the adjacent structure is mainly responsible for the position of the resonant frequency for both modes, i.e., common and differential modes. In contrast, the width of the adjacent structure changes the magnitude of the resonances for both modes.
- Applying a distance of approximately 6 times the substrate thickness reduces the resonant behavior for the frequency range investigated in this study.
- In symmetrical DUTs, the mode conversion losses are less affected by the shape of adjacent structures or the distance to adjacent structures.
- Once asymmetries occur, mode conversion losses are strongly affected by the adjacent structures.

Acknowledgment

References

[1] C. Seguinot, P. Kennis, J.-F. Legier, F. Huret, E. Paleczny, and L. Hayden, "Multimode TRL. A New Concept in Microwave Measurements: Theory and Experimental Verification," *IEEE Transactions on Microwave Theory and Techniques*, vol. 46, no. 5, pp. 536–542, 1998.

[2] M. Wojnowski, V. Issakov, G. Sommer, and R. Weigel, "Multimode TRL Calibration Technique for Characterization of Differential Devices," *IEEE Transactions on Microwave Theory and Techniques*, vol. 60, no. 7, pp. 2220–2247, 2012.

[3] T. D. Pham, D. Allal, F. Ziadé, and E. Bergeault, "On-Wafer Coplanar Waveguide Standards for S-Parameter Measurements of Balanced Circuits Up to 40 GHz," *IEEE Transactions on Instrumentation and Measurement*, vol. 68, no. 6, pp. 2160–2167, 2019.

[4] V. Issakov, M. Wojnowski, A. Thiede, and R. Weigel, "Considerations on the De-embedding of Differential Devices using Two-port Techniques," in *2009 European Microwave Conference (EuMC)*, 2009, pp. 695–698.

[5] F. Ziadé, M. Hudlička, M. Salter, T. Pavlíček, and D. Allal, "Uncertainty Evaluation of Balanced S-parameter Measurements," in *2016 Conference on Precision Electromagnetic Measurements (CPEM 2016)*, 2016, pp. 1–2.

[6] K.-K. Cheng, "Analysis and Synthesis of Coplanar Coupled Lines on Substrates of Finite Thicknesses," *IEEE Transactions on Microwave Theory and Techniques*, vol. 44, no. 4, pp. 636–639, 1996.

[7] G. N. Phung, F. J. Schmückle, R. Doerner, T. Fritzsch, S. Schulz, and W. Heinrich, "Crosstalk Effects of Differential Thin-Film Microstrip Lines in Multilayer Motherboards," in *2019 12th German Microwave Conference (GeMiC)*, 2019, pp. 178–181.

[8] R. B. Marks, "A Multiline Method of Network Analyzer Calibration," *IEEE Trans. on Microwave Theory and Techniques*, vol. 39, no. 7, pp. 1205–1215, 1991.

[9] "CST Studio Suite," 2022. [Online]. Available: https://www.3ds.com/products-services/simulia/products/cst-studio-suite/